International Journal of Biomedicine 12(1) (2022) 24-28
http://dx.doi.org/10.21103/Article12(1)_OA1

ORIGINAL ARTICLE

Radiology

INTERNATIONAL JOURNAL OF BIOMEDICINE

Standardization of a Non-Invasive MRI Assessment of Liver Iron Overload Using a Phantom Containing Superparamagnetic Iron Oxide Nanoparticles

Petr A. Bulanov[1*]; Evelina E. Manzhurtseva[1]; Petr E. Menshchikov[1,2], PhD; Dmitry A. Kupriyanov[1,2], PhD; Galina A. Novichkova[1], PhD, ScD; Galina V. Tereshchenko[1], PhD

[1]Dmitry Rogachev National Medical Research Center of Pediatric Hematology, Oncology and Immunology, Moscow, Russia
[2]Philips Healthcare, Moscow, Russia

Abstract

***Background*:** Liver iron overload is a common diagnosis in patients with frequent blood transfusions. MRI is a promising non-invasive method for assessing liver iron concentration. We have created an MR-compatible phantom to develop a method for the standardization of T2* mapping and following conversion of T2* values (ms) into iron concentration (mg/mL) for an assessment of overload grade.

***Methods and Results*:** The standardization process involved the development of an MR-compatible phantom with solutions of paramagnetic iron oxide nanoparticles of various concentrations mimicking various degrees of liver iron overload. Using this phantom, we assessed the repeatability of T2* values obtained on reference MRI scanners (3T and 1.5T) at the D. Rogachev NMRCPHOI on 6 MRI acquisitions with one-week intervals. To assess the reproducibility of the results obtained on other MRI scanners, we compared these measurements with the reference values.

***Conclusion*:** The method for the standardization of T2* mapping on various 1.5T and 3T MRI scanners was tested. This method is based on the use of our phantom to validate or calibrate (if necessary) the MRI study protocol. The standardization protocol provided an opportunity to use the empirical formula (revealed in our institute as well as in other studies) for converting T2* values from any MRI scanner into LIC (mg/mL). (**International Journal of Biomedicine. 2022;12(1):24-28.**)

Key Words: iron overload • MRI diagnosis • T2* mapping • MRI phantom • SPIO

For citation: Bulanov PA, Manzhurtseva EE, Menshchikov PE, Kupriyanov DA, Novichkova GA, Tereshchenko GV. Standardization of a Non-Invasive MRI Assessment of Liver Iron Overload Using a Phantom Containing Superparamagnetic Iron Oxide Nanoparticles. International Journal of Biomedicine. 2022;12(1):24-28. doi:10.21103/Article12(1)_OA1

Introduction

Iron overload is a condition in which extra iron builds up in organs and tissues, causing toxic damage and, consequently, organ dysfunction. Iron overload may occur due to hereditary hemochromatosis or result from anemia requiring regular transfusions of donor red blood cells.[1] Timely diagnosis of iron overload is essential for the prediction of target organ dysfunction as well as for the planning and monitoring of chelation therapy.[2] Until recently, the only accurate method of iron overload assessment was the analysis of liver samples by atomic absorption spectrometry. Serum ferritin concentration, widely used as an indirect measure of iron stores in patients with hemochromatosis, is not always a reliable indicator of iron status in patients suffering from post-transfusion iron overload. The applicability of liver biopsy is limited by such major negative factors as the invasiveness of the procedure and significant variability in iron concentration due to the small size of specimens and the heterogeneity of iron deposition in the liver.[3] New magnetic resonance imaging (MRI) technologies allow us to quantify iron concentration in the liver, heart, and pancreas using special pulse sequences.[4]

***Corresponding author**: Petr A. Bulanov. Dmitry Rogachev National Medical Research Center of Pediatric Hematology, Oncology and Immunology. Moscow, Russia. E-mail: petepeter@yandex.ru*

The most widely used quantification MRI method is T2* mapping.[5] Iron is stored in the liver parenchyma mainly in two forms: ferric hydroxide bound to ferritin and ferric hydroxide in hemosiderin. Because of the paramagnetic properties of iron, iron-containing substances also exhibit paramagnetic properties. Paramagnets are substances that, because of magnetization in the presence of an external magnetic field (for example, in MRI), generate large inhomogeneities in local magnetic fields and consequently affect T2* relaxation time, which is heavily dependent on such inhomogeneities.[3] T2* is measured by a gradient echo sequence (GRE) with multiple echo times (TEs). The obtained images are used to create a map of T2* value distribution (hereinafter referred to as a "T2* map") that is sensitive to ferritin and hemosiderin concentrations: the lower T2* values, the more iron is present in the area of interest, and the higher iron overload is.[6] This method is non-invasive and allows for a quick assessment of iron overload in the entire liver, thus solving the two major problems associated with liver biopsy at once. However, we cannot replace biopsy with T2* mapping because of the absence of standards for converting T2* values into liver iron concentration (LIC). The creation of the standard is crucially essential for further diagnosis and an accurate assessment of iron overload.

One of the main methods for T2* values to be converted into LIC is an experimental calibration based on T2* mapping and biopsy findings.[7] However, as seen from experience, such calibration curves may be specific to the cause of iron overload as well as to methods used in the experiment (T2* mapping parameters, biopsy techniques, scanners used, etc.).[7] In other words, these restrictions substantially limit using of the calibration curve anywhere except the place where the curve was obtained ("reference MRI scanner"). Nevertheless, using the calibration curves is possible if T2* values acquired on any MRI scanner will be matched with the values from the reference MRI scanner. FerriScan® (Australia) is the most successful attempt at standardization. It is a commercial product approved by the United States Food and Drug Administration (the FDA) to calculate LIC based on T2* values.[8] This technique has demonstrated high reproducibility in multicenter studies.[9] Nevertheless, its wide use is strongly limited by the high cost.

The aim of this study was to develop and validate an effective and simple algorithm that would help test the correspondence between T2* values obtained with various MRI scanners and those obtained with reference 1.5T and 3T MRI scanners at the National Medical Research Center of Pediatric Hematology, Oncology and Immunology named after Dmitry Rogachev by using an MR-compatible phantom containing paramagnetic iron oxide (Fe3O4) nanoparticles. Such an algorithm would allow healthcare facilities to easily start using T2* mapping to assess LIC (based on the conversion curve obtained by us previously[6]) without the necessity of laborious preliminary experimental creation of calibration curves.

Materials and Methods

The Development of a Phantom

The phantom consisted of 28 tubes, 50 ml each, filled with colloid solutions of various concentrations (Fig.1) containing paramagnetic iron oxide nanoparticles (Fe_3O_4). The nanoparticles were produced using the method proposed by Elmore[10]:

$$FeSO_4 7H2O + 2FeCl_3 6H_2O + 8NH_3 H_2O = Fe_3O_4 + 6NH_4Cl + (NH_4)2SO_4 + 23H_2O,$$

where iron(III) chloride hexahydrate and iron(II) sulfate heptahydrate were used as carriers of ferrous and ferric ions, ammonium hydrate was used to precipitate and synthesize the nanoparticles, and citric acid, a surfactant, was used for growth control and stabilization of the particles. The resulting solution was centrifuged at 1500 rpm for 5 minutes to precipitate large particles. The top layer of the solution filtered through standard filter paper with an average pore size of 3 - 5 µm was the colloidal suspension of iron oxide nanoparticles that we had aimed to obtain. The resulting solutions with high iron concentration were diluted to achieve T2* values similar to those seen in a healthy liver and in the four grades of iron overload.[6]

Fig. 1. A. An example of phantom positioning in an MRI scanner. B. The phantom containing superparamagnetic iron oxide nanoparticles (Fe_3O_4)

MRI Scanning and Post-processing

The phantom was scanned using four MRI scanners from different manufacturers and with different field strengths (Table 1).

Table 1.

MRI scanners used in the research

MRI scanner / Magnetic field strength	Maximum gradient strength /slew rate	Reference / Control	Receiver coil
Philips Achieva dStream (Best, The Netherlands) /3T	80 mT/m / 200 T/m/s	Reference 3T MRI scanner NMRCPHOI	dS Torso anterior coil combined with a coil integrated in the table, with 32 channels in total
Philips Achieva (Best, The Netherlands) /3T	80 mT/m / 200 T/m/s	Control 3T MRI scanner CRIEPST	dS Torso anterior coil combined with a coil integrated in the table, with 32 channels in total
Signa GE (Chicago, Illinois, USA)/1.5T	33 mT/m / 120 T/m/	Reference 1.5T MRI scanner NMRCPHOI	8-channel Body Array coil
Philips Ingenia (Best, The Netherlands) /1.5T	45 mT/m / 200 T/m/s	Control 1.5T MRI scanner NMRCTO	16-channel FlexCoverage Anterior coil

The phantom was scanned on the reference MRI scanners at the Dmitry Rogachev National Medical Research Center of Pediatric Hematology, Oncology and Immunology (NMRC PHOI) 6 times with one-week interval. T2* maps acquisition on control MRI scanners in Clinical and Research Institute of Emergency Pediatric Surgery and Traumatology (CRIEPST) and National Medical Research Center of Traumatology and Orthopedics named after N. N. Priorova (NMRCTO). Specifications of the reference and control MRI scanners are presented in Table 1. The MRI protocols included T2* mapping using multi-phase fast gradient echo (*mGRE*). For all the scanners, the main parameters were as follows: the flip angle (FA) - 45°, the echo time (TE) – 1.2 ms, the number of echoes – 20 with ΔTE = 1.5 ms, the repetition time (TR) – 350 ms; the resolution – 1.5×1.5 mm. For MRI scanners with field strengths of 1.5T and 3T, the slice thickness was 10 and 7 mm, respectively.

T2* values were calculated in two ways. One was automatic T2* mapping using integrated commercial software packages. Mean T2* values were measured within the marked regions of interest (ROI) on T2* maps. The other was manual data analysis using free-available conversional tables.[11] T2* values in ROI were computed by exponential approximation of decay curves via the maximum likelihood method.

Statistical Analysis. We calculated mean T2* values and standard deviations for each phantom tube. The statistical analysis was conducted using GraphPad Prism 8.0.1 software. The repeatability and reproducibility of T2* measurements were assessed. Repeatability was defined as the stability of data obtained during several scanning sessions on the same (reference) MRI scanner over a long period of time. To assess repeatability, we also calculated mean coefficients of variation with the following formula:

$$v_x = \frac{\sigma}{\bar{x}} * 100\%$$

Additionally, we evaluated linear correlations between the results obtained by automatic and manual processing (see MRI Scanning and Post-processing).

Reproducibility was defined as the degree of agreement between T2* values obtained on the control MRI scanners and those obtained on the reference scanners using various methods of T2* calculation (see MRI Scanning and Post-processing). To test the reproducibility of the results across different MRI scanners, we estimated the correlation between measurements obtained on the reference and control MRI scanners. Additionally, Bland-Altman plots were created to assess the repeatability and reproducibility of the results visually.

Results

An example of a T2* map (calculated using commercial processing software for Philips 3T MRI scanner) is represented in Figure 2. The ranges of T2* values for 1.5 and 3T MRI scanners were as follows: from 18.4 to 0.7 ms and from 14.1 to 0.5 ms, respectively.

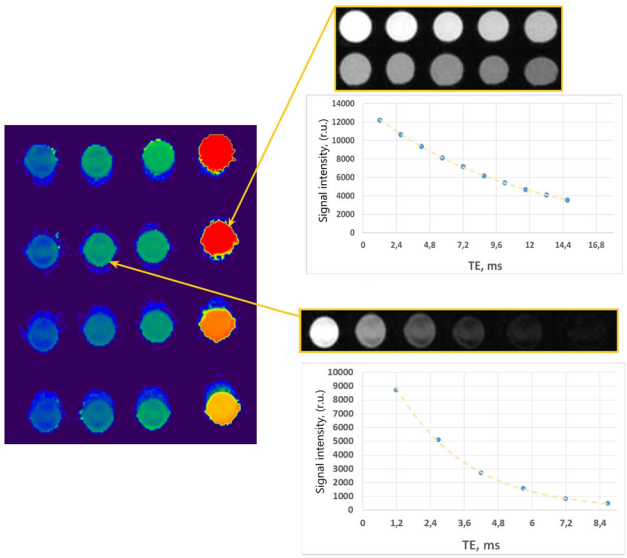

Fig. 2. *An example of a T2* map (on the left) obtained with commercial processing software on the Philips 3T scanner. For two tubes, the examples of T2* signal decay and the dependence of signal intensity (relative units) on TE, ms (TE_1 = 1.2 ms, ΔTE = 1.5 ms) are given. The upper plot was constructed for the tube with the real iron concentration of 0.21 mg/mL and the T2* time = 1.2±0.2 ms, the lower plot was constructed for the tube with the real iron concentration of 0.77 mg/mL and the T2* time = 9±0.2 ms.*

The mean coefficients of variation (C_v) for the reference 1.5 and 3T MRI scanners at our center were 4% and 5%, respectively. The analysis of the repeatability of the technique on the reference MRI scanners is presented in the form of Bland-Altman plots (Fig. 3 A, B). For both scanners, the 95% confidence intervals (CI) ranged from -0.4 to +0.4 ms. Standard deviations for 1.5T and 3T scanners lied in the range of 2% - 5% and 2% - 8%, respectively, whereas in the case of 3T MRI scanner, we observed an increase in the values of standard deviations and a decrease in T2* values.

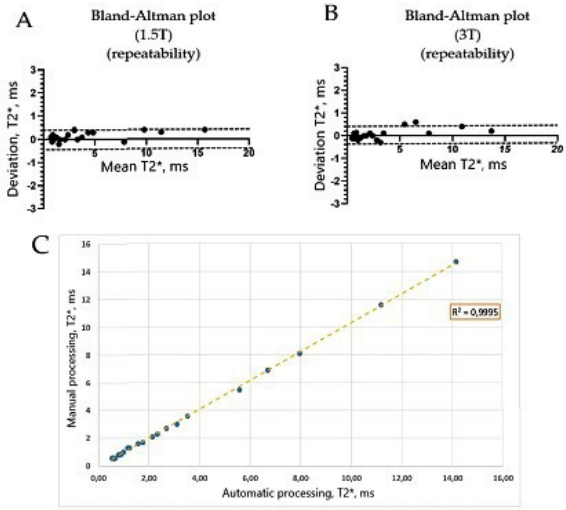

Fig. 3. *Testing the repeatability of the results: Bland-Altman plots for the repeatability of the results obtained on the reference scanners with field strengths of 1.5T (A) and 3T (B), showing the mean deviations of the T2* values (ms) from the average during 6 observations. The correlation between T2* values (ms) obtained by automatic mapping on a Philips 3T scanner and by manual processing of T2* values in ROI (B).*

Furthermore, we found a significant (R^2=0.99, P<0.01) correlation between the T2* values obtained using different calculation methods (Fig. 3B).

We found significant correlations between reference values and the values obtained on other scanners (Fig. 4 A, B): 1.5T - R2 = 0.99 (P<0.01); 3T - R2 = 0.99 (P<0.01). The analysis of the reproducibility of the technique using various MRI scanners is presented in the form of Bland-Altman plots (Fig. 4 C, D). For the scanners with field strengths of 1.5T and 3T, the 95% confidence intervals range from -0.4 to +0.4 ms, respectively.

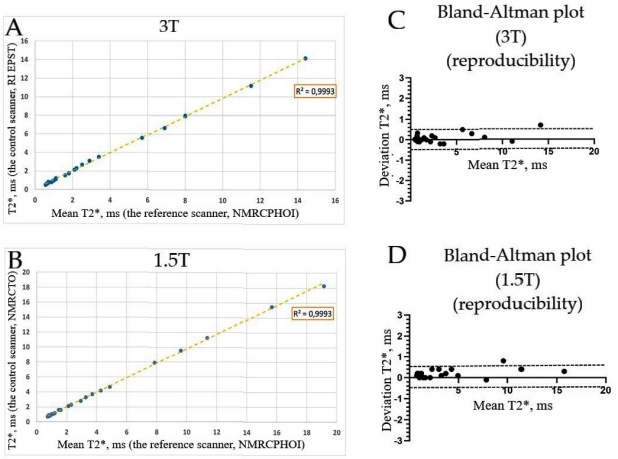

Fig. 4. *Testing the reproducibility of the results: A, B - correlations between the T2* values obtained on reference and other devices with field strengths of 3T and 1.5T, respectively. C, D - Bland-Altman plots for similar T2* values.*

Discussion

In this study, we analyzed the repeatability and reproducibility of an MRI technique for assessing iron overload in the liver based on the application of mGRE pulse sequence, the most available and frequently used technique for measuring iron overload. The coefficients of variation for 6 repeated measurements obtained over one and a half months from MRI scanners at the D. Rogachev NMRCPHOI were less than 5%, indicating excellent repeatability of T2* measurements on both scanners. These results are also confirmed by the statistical analysis and Bland-Altman plots. A significant correlation between T2* values calculated using different methods suggests that one is free to choose any way to process data obtained from the same MRI scanner.

The mean standard deviations show that relative errors of T2* increase proportionally to an increase in iron concentration in a tube due to faster signal decay at a higher iron concentration and, consequently, fewer points for the approximation used to determine T2* values. The lower the field strength is, the slower the T2* relaxation process occurs (which also explains the difference between T2* values). Therefore, T2* measurement errors turn out to be smaller at 1.5T field strength than at 3T. Still, this error associated with using 3T field strength scanners is not critical. It lies within confidence intervals (95%) for mean values obtained at 1.5T, which means that 3T MRI scanners can be successfully applied to detect iron overload. To reduce T2* measurement errors at 3T, ultra-short echo time (UTE) sequences can be used.[12] This technique provides the opportunity to reduce the initial TE value and thus to obtain more points for the approximation at high iron concentrations and to increase the accuracy of the approximation and the reliability of the results. Moreover, radial data collection used in the uTE sequence allows us to avoid respiratory motion artifacts,[13] providing the opportunity to use the free-breathing sequence,[14] which is undoubtedly essential when working with young children.

The results of reproducibility testing also suggest that the created phantom retains all necessary characteristics (homogeneity and the constancy of concentrations and its paramagnetic properties) during a long period of time and, thus, can be used for further evaluation of the reproducibility of T2* calculations on other scanners or with other scanning modes. In contrast to the previous attempts to create phantoms for T2* measurements,[15,16] in this study, we chose superparamagnetic iron oxide Fe3O4 (SPIO) nanoparticles as a paramagnetic material, since hemosiderin contains colloidal particles of ferric hydroxide.[17]

Using the phantom, we tested the reproducibility of the T2* values on MRI scanners from other institutions and compared them with the values obtained on the reference scanners. Based on the correlation and Bland-Altman analyses, T2* mapping techniques used on the 3T and 1.5T control MRI scanners demonstrated good reproducibility. As a result, the T2* measurements were consistent across various devices (lied within the 95% confidence interval). This result clearly indicates that the previously developed formulas for the conversion of T2* values into LIC can be used for these scanners as well. It should be considered that the mapping parameters were selected to be as similar as possible to those that we used on the reference scanner. The modification of the most parameters should not significantly change the calculated T2* values; however, the choice of TE values for the mGRE and uTE sequence should be very careful, since different sets of TE times can strongly affect the calculated T2* values due to the phase effects between fat and water signals.[5]

Thus, to use the previously obtained curves to convert T2* values into LIC, [4,6] it will be sufficient to test the correspondence of T2* values using the phantom we created. In case of any discrepancies, the scanning protocol should be modified until this concordance is obtained. Our experience gained in this study showed that good concordance could be obtained using scanners from different manufacturers, which was also confirmed by the previous studies.

The standardization protocol created in the following study provided an opportunity to use the empirical formula for converting T2* values into LICm that has been developed in our institute[4,6] as well as for other calibration curves [18,19] for any MRI scanners.

As a result of this study, the method for the standardization of T2* mapping on various 1.5T and 3T MRI scanners was tested. This method is based on the use of our MR-compatible phantom. Using this phantom allows for a quick and effective comparison of obtained T2* values against

the reference values and for calibration (if necessary). Liver iron overload can thus be measured without prior long-term validation of T2* mapping and conversion of T2* values (ms) into LIC (mg/mL).

Acknowledgments

We thank Prof. Akhadov T.A. from Clinical and Research Institute of Emergency Pediatric Surgery and Traumatology and Prof. Morozov A.K. from and National Medical Research Center of Traumatology and Orthopedics named after N.N. Priorova for the phantom acquisition sessions on MRI scanners.

Competing Interests

The authors declare that they have no competing interests.

References

1. Siah CW, Trinder D, Olynyk JK. Iron overload. Clin Chim Acta. 2005 Aug;358(1-2):24-36. doi: 10.1016/j.cccn.2005.02.022.
2. Smetanina NS. [Current possibilities of chelation therapy]. Russian Journal of Pediatric Hematology and Oncology. 2014;(1):51-61. doi: 10.17650/2311-1267-2014-0-1-51-61. [Article in Russian].
3. Labranche R, Gilbert G, Cerny M, Vu KN, Soulières D, Olivié D, Billiard JS, Yokoo T, Tang A. Liver Iron Quantification with MR Imaging: A Primer for Radiologists. Radiographics. 2018 Mar-Apr;38(2):392-412. doi: 10.1148/rg.2018170079.
4. Nazarova EE, Kupriyanov DA, Novichkova GA, Tereshchenko GV. [Noninvasive assessment of iron overload by magnetic resonance imaging]. Pediatric Hematology/Oncology and Immunopathology. 2020;19(3):158-163. doi: 10.24287/1726-1708-2020-19-3-158-163. [Article in Russian].
5. Hernando D, Levin YS, Sirlin CB, Reeder SB. Quantification of liver iron with MRI: state of the art and remaining challenges. J Magn Reson Imaging. 2014 Nov;40(5):1003-21. doi: 10.1002/jmri.24584.
6. Nazarova EE, Tereshchenko GV, Abakumov MA, Smantser VA, Kupriyanov DA, Smetanina NS. [MRI T2*-mapping for liver iron assessment in pediatric patients with secondary iron overload]. Pediatric Hematology/Oncology and Immunopathology. 2017;16(3):23-27. doi: 10.24287/1726-1708-2017-16-3-23-27.[Article in Russian].
7. Garbowski MW, Carpenter JP, Smith G, Roughton M, Alam MH, He T, Pennell DJ, Porter JB. Biopsy-based calibration of T2* magnetic resonance for estimation of liver iron concentration and comparison with R2 Ferriscan. J Cardiovasc Magn Reson. 2014 Jun 10;16(1):40. doi: 10.1186/1532-429X-16-40.
8. St Pierre TG, Clark PR, Chua-anusorn W, Fleming AJ, Jeffrey GP, Olynyk JK, Pootrakul P, Robins E, Lindeman R. Noninvasive measurement and imaging of liver iron concentrations using proton magnetic resonance. Blood. 2005 Jan 15;105(2):855-61. doi: 10.1182/blood-2004-01-0177.
9. St Pierre TG, El-Beshlawy A, Elalfy M, Al Jefri A, Al Zir K, Daar S, Habr D, Kriemler-Krahn U, Taher A. Multicenter validation of spin-density projection-assisted R2-MRI for the noninvasive measurement of liver iron concentration. Magn Reson Med. 2014 Jun;71(6):2215-23. doi: 10.1002/mrm.24854.
10. Gubin SP, Koksharov YuA, Khomutov GB, Yurkova GYu. Magnetic nanoparticles: preparation, structure and properties. Russ Chem Rev. 2005;74(6):489-520. doi: 10.1070/RC2005v074n06ABEH000897. [Article in Russian].
11. Fernandes JL, Fioravante LAB, Verissimo MP, Loggetto SR. A free software for the calculation of T2* values for iron overload assessment. Acta Radiol. 2017 Jun;58(6):698-701. doi: 10.1177/0284185116666416.
12. Doyle EK, Toy K, Valdez B, Chia JM, Coates T, Wood JC. Ultra-short echo time images quantify high liver iron. Magn Reson Med. 2018 Mar;79(3):1579-1585. doi: 10.1002/mrm.26791.
13. Haacke EM, Brown RF, Thompson M, Venkatesan R. Magnetic resonance imaging: Physical principles and sequence design. New York: J. Wiley & Sons. 1999.
14. Zhu X, Chan M, Lustig M, Johnson KM, Larson PEZ. Iterative motion-compensation reconstruction ultra-short TE (iMoCo UTE) for high-resolution free-breathing pulmonary MRI. Magn Reson Med. 2020 Apr;83(4):1208-1221. doi: 10.1002/mrm.27998.
15. Mobini N, Malekzadeh M, Haghighatkhah H, Saligheh Rad H. A hybrid (iron-fat-water) phantom for liver iron overload quantification in the presence of contaminating fat using magnetic resonance imaging. MAGMA. 2020 Jun;33(3):385-392. doi: 10.1007/s10334-019-00795-7.
16. Hines CD, Yu H, Shimakawa A, McKenzie CA, Brittain JH, Reeder SB. T1 independent, T2* corrected MRI with accurate spectral modeling for quantification of fat: validation in a fat-water-SPIO phantom. J Magn Reson Imaging. 2009 Nov;30(5):1215-22. doi: 10.1002/jmri.21957.
17. Saito H, Hayashi H. Transformation rate between ferritin and hemosiderin assayed by serum ferritin kinetics in patients with normal iron stores and iron overload. Nagoya J Med Sci. 2015 Nov;77(4):571-83.
18. Wood JC, Enriquez C, Ghugre N, Tyzka JM, Carson S, Nelson MD, Coates TD. MRI R2 and R2* mapping accurately estimates hepatic iron concentration in transfusion-dependent thalassemia and sickle cell disease patients. Blood. 2005 Aug 15;106(4):1460-5. doi: 10.1182/blood-2004-10-3982.
19. Storey P, Thompson AA, Carqueville CL, Wood JC, de Freitas RA, Rigsby CK. R2* imaging of transfusional iron burden at 3T and comparison with 1.5T. J Magn Reson Imaging. 2007 Mar;25(3):540-7. doi: 10.1002/jmri.20816.